LANGMUIR

pubs.acs.org/Langmuir Article

Programmable Morphology Evolution of Rod-Coil-Rod Block Copolymer Assemblies Induced by Variation of Chain Ordering

Xiao Jin,[†] Fangsheng Wu,[†] Jiaping Lin,* Chunhua Cai,* Liquan Wang, Jianding Chen, and Liang Gao

Cite This: *Langmuir* 2021, 37, 3148–3157 Read Online

ACCESS | Metrics & More | Article Recommendations | Supporting Information

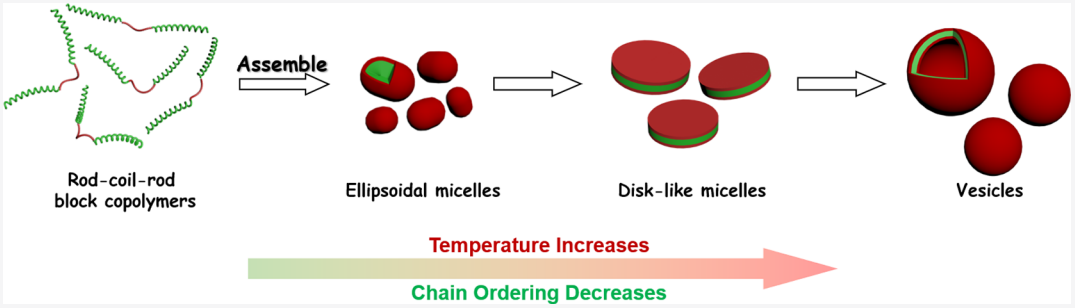

ABSTRACT: Morphology transition of block copolymer assemblies in response to external stimuli has attracted considerable attention. However, our knowledge about the mechanism of such a transition is still limited, especially for rod-coil block copolymers. Here, we report a programmable morphology evolution of assemblies induced by variation of chain ordering for rod-coil-rod triblock copolymers. A sequence of morphology transition from ellipsoids to disks, bowls, and vesicles is observed by increasing the solution temperature. At high temperatures, the mobility of the rod chain increases and the rigidity of the rod chain decreases. This gives rise to an ellipsoid-to-vesicle morphology transition. Dissipative particle dynamics theoretical simulations were performed to reveal the mechanism of this morphology transition process. It was found that the increase of rod chain mobility and the decrease of rod chain rigidity induce a decrease of chain ordering of rod blocks as temperature increases, which results in an ellipsoid-to-vesicle morphology transition. The gained information can guide the construction of nanoassemblies based on the rod-coil block copolymers.

INTRODUCTION

In biological systems, biomacromolecules can form diverse nanostructures and the stimuli-response behaviors of these nanostructures are of great importance for life.[1] Similarly, synthetic polymers are capable of assembling into diverse nanostructures, and the design of polymeric assemblies in response to external stimuli has attracted significant interest. Manipulating the morphology of synthetic polymeric assemblies is not only significant for understanding the biological process but also important for the preparation of intelligent materials in applications of nanoreactors, drug delivery, cosmetics, and so forth.[2−6] Given the important role of assembly morphologies in determining various potential applications, a series of strategies have been developed to achieve the morphology transition of polymeric assemblies.

So far, various stimuli including temperature, pH, salt, light, and enzyme have been applied to regulate the morphology transition of block and graft copolymer assemblies.[7−14] Among diverse external stimuli, the temperature has attracted particular attention due to the precise regulation *in vitro* with precise control in time and space.[15−23] Usually, temperature-induced morphology transitions are primarily achieved by the change of chain amphiphilicity, as the hydrophilic/hydrophobic balance is thermoresponsive and crucial for the morphology of copolymer assemblies.[16] For example, poly(*N*-isopropyl acrylamide) (PNIPAm) bearing lower critical solution temperature (LCST) property is a typical thermoresponsive polymer, and the PNIPAm-based copolymer assemblies can achieve thermal-induced morphology transitions by altering temperature around the LCST.[22] Note that the LCST property refers to a significant variation of the solvation degree in a solution under a small temperature shift. A minor variation of the solvation degree of a polymer can influence the self-assembly behavior of block copolymers. For instance, Armes et al. found that poly(stearyl methacrylate)-*b*-poly(benzyl methacrylate) (PSMA-*b*-PBzMA) copolymer assemblies can achieve a vesicle-to-worm transition by increasing the temperature, which is attributed to the greater

Received: December 27, 2020
Revised: February 16, 2021
Published: March 4, 2021

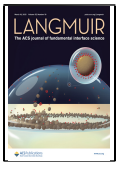

https://dx.doi.org/10.1021/acs.langmuir.0c03644
Langmuir 2021, 37, 3148–3157

solvation of the PBzMA core-forming blocks at higher temperatures.[17] Zhao et al. report a temperature-dependent sphere-to-nanoribbon morphology transition of aggregates assembled from heterografted polymers comprising the poly(styrene-*co*-maleimide) backbone and heterografts of poly(2-(dimethylamino)ethyl methacrylate) (PDMA), which is induced by the decrease of the hydration degree of PDMA chains at a higher temperature.[21] Despite these advances in temperature-induced self-assembly, it is still fascinating to explore novel systems to achieve controllable morphologies among diverse nanostructures.

In contrast to well-studied coil−coil block copolymers, the rod-coil copolymers exhibit complicated self-assembly features because of the ordered packing manner of rod blocks in the aggregate core.[24−36] Thus, the change of chain ordering of rod blocks can be an important factor regulating the morphology of rod-coil copolymer assemblies. For instance, the chain ordering of rod blocks can be destroyed by the rod-to-coil conformation change which is usually achieved by varying the pH or initial solvent. The chain ordering change thus brings out a morphology transition.[27,30] As a matter of fact, the temperature can also manipulate the chain ordering of rigid polymers in the aggregate structure such as the homopolymer liquid crystal (LC), thereby influencing the aggregate structures.[32] This external stimulus may cause the morphology transition of rod-coil block copolymer assemblies in solution as well. However, so far, limited attention is focused on the temperature-dependent morphology transition of the rod-coil copolymer assemblies; especially, the underlying mechanism is not well understood.

Apart from the experimental studies, theoretical simulations have become a powerful tool to investigate the self-assembly behaviors of block copolymers, which break through the experimental limitations and provide a novel perspective.[37−49] By combining theoretical simulations with experimental results, the essential features and mechanism of the self-assembly system can be well revealed. For example, Jiang et al. report the kinetics of vesicle formation of amphiphilic triblock copolymers by combining experiments and dissipative particle dynamics (DPD) simulations.[37] DPD simulation has reproduced the assembling behavior in experiments and reveals that the pathway difference for spontaneous vesicle formation can be attributed to the existence of many metastable states in the system.

Herein, we report a programmable morphology transition of poly(γ-benzyl L-glutamate)-*block*-poly(ethylene glycol)-*block*-poly(γ-benzyl L-glutamate) (PBLG-*b*-PEG-*b*-PBLG) rod-coil-rod triblock copolymer assemblies in response to temperature. Ellipsoids are formed at room temperature. As temperature increases, the aggregate morphologies evolve into disks, bowls, and vesicles in sequence. During the transition process, the chain mobility increases, and the chain rigidity decreases. Additionally, DPD simulation was performed to provide detailed information such as chain ordering variation that cannot be directly observed experimentally. By combining experiments with theoretical simulations, the mechanism of such a temperature-dependent morphology transition is suggested.

EXPERIMENTS AND SIMULATION METHOD

Synthesis of PBLG-*b*-PEG-*b*-PBLG Triblock Copolymers. PBLG-*b*-PEG-*b*-PBLG (BEB) triblock copolymers were synthesized by ring-opening polymerization of BLG−NCA initiated by the NH_2−PEG−NH_2 macroinitiator in anhydrous 1,4-dioxane solution. Under a dry nitrogen atmosphere, the reaction was performed in a flame-dried reaction bottle for 3 days at 15 °C. The reaction mixture was poured into a large volume of anhydrous ethanol at the end of polymerization. The precipitates were collected and dried under vacuum; the products were then purified twice by repeatedly precipitating from a chloroform solution into a large volume of anhydrous methanol. The block copolymers were characterized by ^{1}H NMR and GPC testing. Since the degree of polymerization (DP) of the PEG block is known (45), the DP of the PBLG block is determined to be 128 according to ^{1}H NMR results. The copolymer is therefore denoted as $PBLG_{128}$-*b*-PEG_{45}-*b*-$PBLG_{128}$, and the GPC testing gives a polydispersity index (Đ) of the block copolymers of 1.25. Details of the synthesis and characterization for the triblock copolymers are presented in Section 1.1 of the Supporting Information.

Preparation of Aggregate Solutions. PBLG-*b*-PEG-*b*-PBLG block copolymers were dissolved in tetrahydrofuran (THF), and the polymer concentration was 0.1 g/L. To 1 mL of the polymer solution, 0.3 mL of deionized water was slowly added in 10 min with vigorous stirring. After adding the deionized water, the transparent solution became tint blue, which indicated the formation of aggregates. To remove the organic solvent, the solution was dialyzed against deionized water for at least 3 days. The experiments were carried out at various temperatures from 20 to 60 °C. Details of sample preparation are presented in Section 1.2 of the Supporting Information.

Characterization of the Assemblies. The morphologies of the assemblies were characterized by various electron microscopes. Scanning electron microscope (SEM) images were obtained by a field emission SEM (S4800, Hitachi) at an accelerating voltage of 15 kV and current of 10 A. The sample was prepared by dropping a drop of solution on a silicon wafer and then drying it at room temperature. The samples were sputtered by platinum before characterization. The transmission electron microscope (TEM) images were examined by the JEM-1400 (JEOL) instrument at an accelerating voltage of 100 kV. The morphologies of the assemblies were also obtained by the XE-100 atomic force microscope (AFM) instrument (Park Systems) with the noncontact mode at room temperature in air. Dynamic light scattering (DLS) and static light scattering (SLS) measurements were carried out on a commercial laser light scattering spectrometer (ALV/CGS-5022) to obtain the hydrodynamic radius R_h and the radius of gyration R_g, respectively. The instrument was equipped with an ALV-High QE APD detector and an ALV-5000 digital correlator using a He−Ne laser (the wavelength λ = 632.8 nm) as the light source. Detailed information is shown in Section 1.3 of the Supporting Information.

DPD Simulations. The DPD method adopted in the present work is a particle-based mesoscopic simulation technique. In the method, several neighboring molecules are coarse-grained into a single particle which moves to obey Newton's equations of motion, $d\mathbf{r}_i/dt = \mathbf{v}_i$ and $m_i d\mathbf{v}_i/dt = \mathbf{f}_i$. The total force $\mathbf{f}_i$ acting on the i-th bead consists of conservative force ($\mathbf{F}_{ij}^C$), dissipative force ($\mathbf{F}_{ij}^D$), and random force ($\mathbf{F}_{ij}^R$), that is, $\mathbf{f}_i = \sum_{j\neq i}(\mathbf{F}_{ij}^C + \mathbf{F}_{ij}^D + \mathbf{F}_{ij}^R)$. In the present work, based on the molecular information of the $PBLG_{128}$-*b*-PEG_{45}-*b*-$PBLG_{128}$ triblock copolymers synthesized in the experiments, a coarse-grained symmetric rod-coil-rod triblock copolymer was constructed. The triblock copolymer model consists of twelve **R** beads for each rod block and four **C** beads for each coil block (denoted by $\mathbf{R}_{12}\mathbf{C}_4\mathbf{R}_{12}$). **R** beads denote the PBLG rigid blocks and **C** beads represent the flexible PEG blocks. The solvent bead was modeled as a single bead (denoted by **S**). The particle density ρ is set to 3. The concentration of copolymers is set as 7.5%. The units of length, time, mass, and energy in the simulations were scaled by r_c, τ, m, and k_BT, respectively. Detailed descriptions of the methods are presented in Section 2.1 of the Supporting Information.

All simulations were performed in 60 × 60 × 60 r_c^3 cubic boxes under the periodic boundary conditions. The equations of motion were integrated by a modified velocity-Verlet algorithm with time step $\Delta t = 0.02\tau$, where time unit $\tau = (mr_c^2/k_BT)^{1/2}$. To mimic the process of morphology transition, the simulation conditions were changed

https://dx.doi.org/10.1021/acs.langmuir.0c03644
Langmuir 2021, 37, 3148−3157

correspondingly which represents the whole heating process from 20 to 60 °C. Every case was carried out by at least 1×10^6 DPD steps. To guarantee that the observations were not accidental, the simulations were carried out with different initial random configurations. The detailed information can be found in Section 2.2 of the Supporting Information.

RESULTS AND DISCUSSION

Morphology Evolution with the Variation of Temperatures. The self-assemblies of PBLG-*b*-PEG-*b*-PBLG (BEB) copolymers were prepared by a selective precipitation method. The experiments were carried out at various temperatures from 20 to 60 °C. The morphologies of the aggregates are characterized by SEM (Figure 1), AFM (Figure S2), and

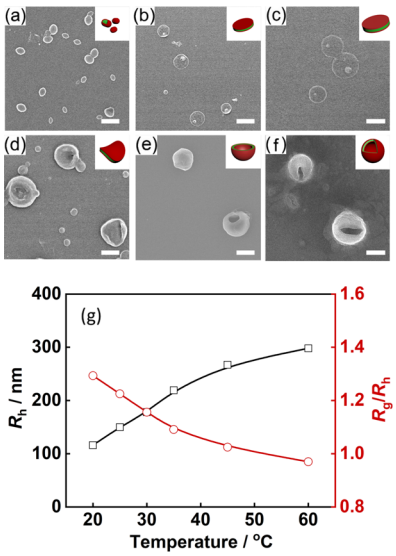

Figure 1. Temperature-dependent morphology transition of BEB copolymer assemblies from ellipsoid to vesicle: (a) ellipsoids at 20 °C, (b) disk-like micelles at 25 °C, (c) larger disk-like structures at 30 °C, (d) bended disk at 35 °C, (e) bowl-like structures at 45 °C, (f) vesicles at 60 °C. The insets show schematic illustrations of each morphology. The green and red parts denote PBLG blocks and PEG blocks, respectively. (g) Plots of R_g/R_h and R_h for the assemblies formed at different temperatures. Scale bars = 300 nm.

TEM (Figure S3). Figure 1a shows the SEM image of the ellipsoids formed at 20 °C. The average length and width of the ellipsoids are about 133 and 98 nm, respectively. When the preparation temperature is increased to 25 °C, disk-like structures are formed (Figure 1b). The mean diameter of the disks is 306 nm, and the height of the disks is around 45 nm (Figure S2f). Larger disks can be obtained at 30 °C (Figure 1c). Further increasing the temperature to 35 °C, curved disks emerge (Figure 1d). When the preparation temperature reaches 45 °C, bowl-shaped structures are formed, and the diameter and height of bowls are around 488 nm (Figure 1e) and 120 nm, respectively (Figure S2g). Eventually, vesicles with a diameter of around 546 nm are observed at 60 °C (Figure 1f).

To better understand the temperature-dependent morphology evolution in solution, we performed DLS as well as SLS experiments to characterize the morphologies. The apparent hydrodynamic radius (R_h) for each aggregate is shown in Figure 1e. The R_h of these aggregates increases from around 110 nm to nearly 300 nm, which verifies the size variation trend of aggregates observed in microscopy images. Additionally, the morphology change can be monitored by the ratio of the average radius of gyration (R_g) to R_h. Generally, the R_g/R_h value of spherical aggregates is in the range of 0.77 (solid sphere) and 1 (vesicle). For nonspherical aggregates, the R_g/R_h value is usually larger than 1.[22] As shown in Figure 1e, the R_g/R_h value of the aggregates formed at 20 °C is 1.29, which corresponds to the ellipsoid structures.[26] When the temperature increases to 60 °C, the R_g/R_h value of the aggregates decreases to 0.96, which indicates the vesicle structures. The *in situ* light scattering results correspond well with the morphology evolution process observed by electron microscopes. The influence of drying on the sample morphology during the specimen preparation can be ruled out. Note that the 2D disk-like micelles can be well captured at a specific temperature. This finding indicates that the polypeptide copolymers are favorable for the formation of 2D assemblies. According to the literature, the R_g/R_h value of 2D structures is usually between 1.0 and 1.5.[33] In the present work, the R_g/R_h value of the 2D aggregates formed at 25 °C is 1.22, which well agrees with the reported data.

Mechanism of Temperature-Dependent Morphology Evolution. As well known, in concentrated solutions, polypeptide homopolymers can form LC structures. The change of chain packing manner in the LC structure can be induced by increasing temperature.[34] The high concentration of polypeptide chains within the micelle core can endow the polypeptide assemblies with unique LC-like properties.[35] Therefore, it is reasonable to deduce that the reason for the present programmable morphology evolution of polypeptide assemblies can be related to the change of chain ordering in response to temperature. Temperature usually influences the mobility of the polymer chains, and the chains become mobile by increasing the temperature.[21] Additionally, the chain rigidity of the PBLG rod block can be decreased at higher temperatures.[30] Based on these speculations, the change of chain mobility and rigidity can be two important factors that cause the variation of chain ordering at different temperatures, which eventually induce morphology changes.

To verify this assumption, we performed two control experiments. First, we examined the influence of chain mobility on the morphology transition. The chain mobility can be increased by decreasing the attraction between PBLG chains. Note that the phenyl groups play an important role in the interaction between the PBLG chains, we replaced the phenyl group in the PBLG block with ethyl groups to reduce the interaction between the BEB copolymers.[29] The chemical formulas of BEB and BEB-Et block copolymers are shown in Figure 2a. ^{1}H NMR characterized the BEB copolymers before (BEB) and after (BEB-Et) modification. As shown in Figure 2b, all signal characteristics of PBLG and PEG blocks are visible. In addition, the signals at $\delta = 4.2$ ppm and $\delta = 1.2$ ppm, which are ascribed to the ethyl group, appear as shown in the dotted boxes. Then, assemblies were prepared from both BEB and BEB-Et at room temperature. The TEM images show that the BEB copolymers self-assemble into ellipsoids as expected (Figure 2c). However, the BEB-Et copolymers form vesicles rather than ellipsoids under the same condition (Figure 2d). According to the above results, the increase of PBLG chain mobility at higher temperatures can be one reason for the ellipsoid-to-vesicle morphology transition.

Second, we examined the effect of polypeptide chain rigidity on the morphology transition of the block copolymers. In the

https://dx.doi.org/10.1021/acs.langmuir.0c03644
Langmuir 2021, 37, 3148−3157

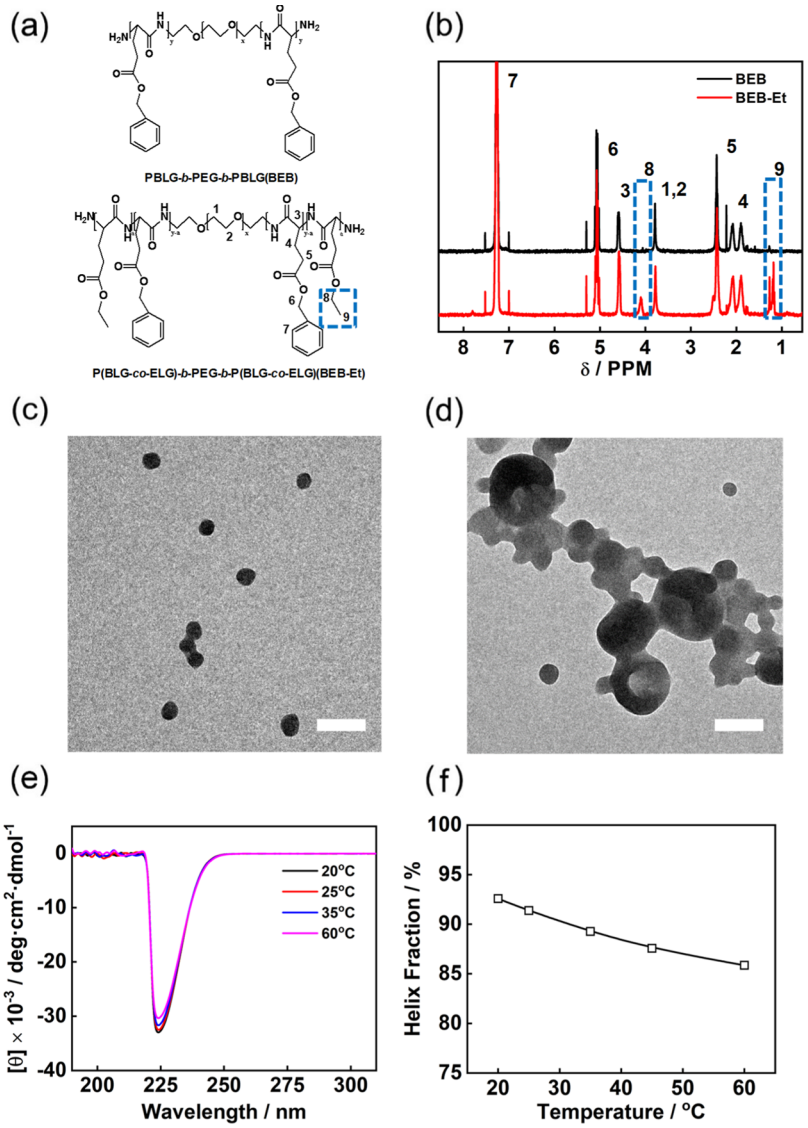

Figure 2. Effect of chain mobility and rigidity of polypeptide on copolymer assemblies at different temperatures. (a) Chemical formulas of the BEB and BEB-Et block copolymers, (b) ^{1}H NMR of the BEB copolymers before and after substituting the phenyl group with the ethyl group (blue dotted boxes represent the position of the characteristic peak of the ethyl group), (c,d) Typical TEM images of ellipsoids and vesicles formed by BEB and BEB-Et copolymers at room temperature, (e) CD spectra of the BEB copolymer dissolved in the THF solvent at different temperatures, (f) temperature dependence of helix fraction for BEB in THF. Scale bars = 400 nm.

polypeptide system, the rigid nature of the polypeptide chain is mainly ascribed to α-helix conformation.[36] We performed circular dichroism (CD) experiment to measure the change of α-helix conformation of the PBLG-*b*-PEG-*b*-PBLG chain in THF at various temperatures. The spectra in Figure 2e shows peaks in the negative region at a wavelength around 222 nm, which indicates the α-helix conformation of PBLG. At higher temperatures, the intensity of this band slightly decreases, which suggests the slight decrease of α-helix content. (Details of the measurement of the helix fraction are shown in Section 1.6 of Supporting Information and Table S1). Figure 2f shows the decrease of the helix fraction of PBLG chains with increasing temperature. The helicity of PBLG blocks at 20 °C is 92.5%. With increasing temperature, the helicity of PBLG blocks decreases to 91.3% (25 °C) and 85.8% (60 °C), which suggests the slight decrease of chain rigidity of PBLG blocks in the investigated temperature range. Note that the content of α-helix conformation is still more than 85% at 60 °C, which indicates that the PBLG blocks still maintain their rigid nature. To further evaluate the rigidity variation of PBLG blocks, R_h of PBLG homopolymers in THF at different temperatures was also characterized by DLS (Figure S4). It is found that the R_h value of the PBLG homopolymers slightly decreases with increasing temperature, which is consistent with the result of the CD experiment. These results indicate that the PBLG chain rigidity decreases at high temperatures. When the rod PBLG chains become flexible, the chain ordering can be broken.[27] As a result, an ellipsoid-to-vesicle morphology transition can be induced.

Chain Ordering Variation during the Morphology Transition Revealed by Theoretical Simulations. From the above experimental results, we learn that the variation of chain mobility and rigidity are responsible for the changes in the aggregate morphology. Due to the limitation of experimental methods, the details of chain behaviors are hard to be observed, and theoretical simulations can be a

https://dx.doi.org/10.1021/acs.langmuir.0c03644
Langmuir 2021, 37, 3148−3157

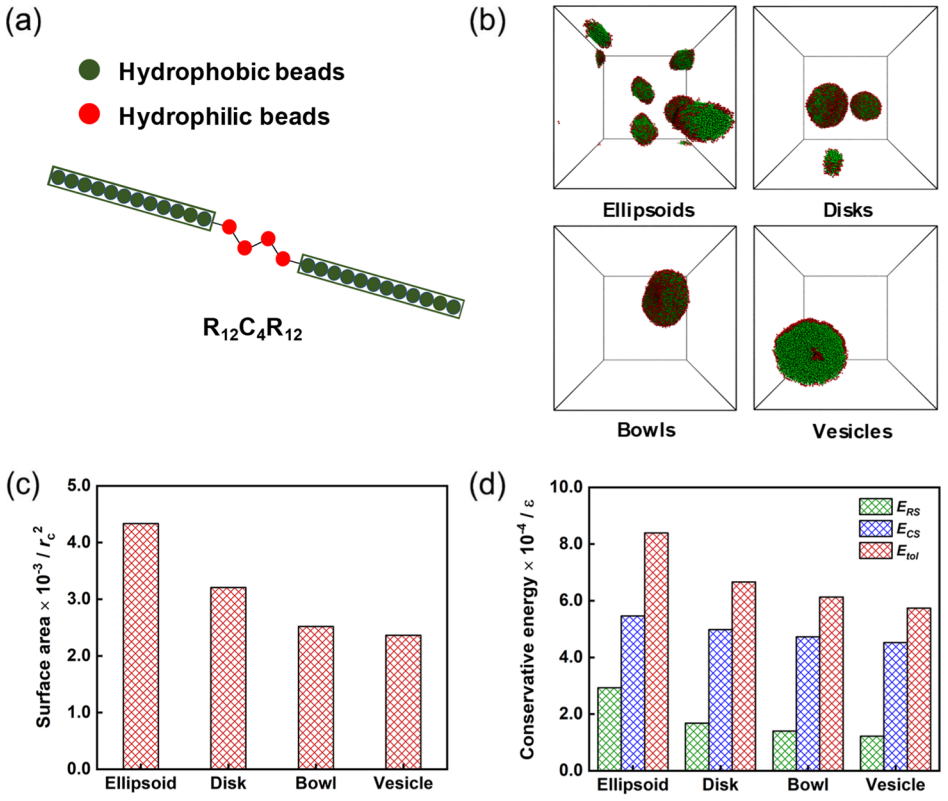

Figure 3. Theoretical simulation of the ellipsoid-disk-bowl-vesicle transition of rod-coil-rod copolymer assemblies. (a) DPD model of the rod-coil-rod triblock copolymer (denoted by $\mathbf{R}_{12}\mathbf{C}_4\mathbf{R}_{12}$). (b) Representative snapshots of the aggregates assembled from rod-coil-rod triblock copolymers at different temperatures: ellipsoids (k_c = 50, k_BT = 0.99), disks (k_c = 48, k_BT = 1.00), bowls (k_c = 46, k_BT = 1.02), and vesicles (k_c = 40, k_BT = 1.11), respectively. (c) Change of surface area during the morphology transitions. (d) Change of conservative energy between copolymers and solvent during the morphology transitions.

powerful tool to support the experimental findings.[37−49] In the present work, DPD simulations are performed to examine the detailed chain mobility and rigidity in various morphologies at the corresponding temperature. The PBLG-*b*-PEG-*b*-PBLG copolymers are mapped into coarse-grained rod-coil-rod copolymer chains in the DPD simulations (Figure 3a). The coarse-grained model consists of twelve **R** beads for each rod block and four **C** beads for each coil block (denoted by $\mathbf{R}_{12}\mathbf{C}_4\mathbf{R}_{12}$). The rod blocks and the coil blocks represent the rigid PBLG blocks and the PEG blocks, respectively. The rod blocks are linearly arranged and treated as rigid bodies, while the coil blocks are modeled as flexible chains. The solvents in the solution are denoted by **S** beads. The interaction parameters between DPD beads are represented by the repulsion parameter of a_{ij}. The neighboring beads in the copolymers are connected *via* the harmonic spring force. The rigidity of the rod blocks is controlled by a three-body angle potential, $U_{ijk}^{c} = 1/2k_c(\cos(\theta) - \cos(\pi))^2$. Details of the DPD method, simulation model, and the simulation parameter settings can be found in Sections 2.1−2.2 in the Supporting Information.

To simulate the increase of temperature from 20, 25, 35, to 60 °C in the experiments, k_BT are set as 0.99, 1.00, 1.02, and 1.11, and k_c are set as 50, 48, 46, and 40, respectively. As shown in Figure 3b, when the temperature is low (k_BT = 0.99, k_c = 50), small ellipsoids can be obtained. The small ellipsoids turn to small disks with increasing temperature (k_BT = 1.00, k_c = 48). Further increasing the temperature (k_BT = 1.02, k_c = 46), small disks fuse into large disks and curve into bowl-like aggregates. Eventually, at higher temperatures (k_BT = 1.11, k_c = 40), the bowl-like aggregates close and vesicles are formed. Thus, the ellipsoid-disk-bowl-vesicle morphology transitions at various temperatures are well reproduced in simulations by tunning the mobility of copolymers and rigidity of rod blocks.

To get an insight into the morphology transitions, the surface areas of the four representative assemblies are evaluated. The surface area of these assemblies is defined as the sum of the areas of all surfaces in the simulation box (*i.e.*, ellipsoids, disks, bowls, and vesicles) and is evaluated through Delaunay triangulation of a 3D point set of the copolymer beads. Surface change usually occurs during morphology transitions.[55] As shown in Figure 3c, for the ellipsoids formed at a low temperature, the surface area is large. As the temperature increases, the ellipsoids fuse into disks leading to a decrease of surface area. The following two processes of disks curving into bowls and bowl closing (vesicle forming) also give rise to the loss of some surface area. The result indicates that variation in temperature drives the assemblies to reduce the surface area in the morphology transition pathway. Generally, vesicle forms when the energy loss due to surface tension effects is too large.[50,51] Due to the complex self-assembly process as well as morphology transitions, the exact surface tension is difficult to be evaluated. Thus, we calculate conservative energy change during the morphology transitions to examine the driving force for the entire process. The conservative energy can be calculated by $\sum_{i>j} 1/2a_{ij}(r_c - r_{ij})^2$ where a_{ij} and r_{ij} are the interaction strength and distance between i and j beads, respectively. The total conservative

https://dx.doi.org/10.1021/acs.langmuir.0c03644
Langmuir 2021, 37, 3148−3157

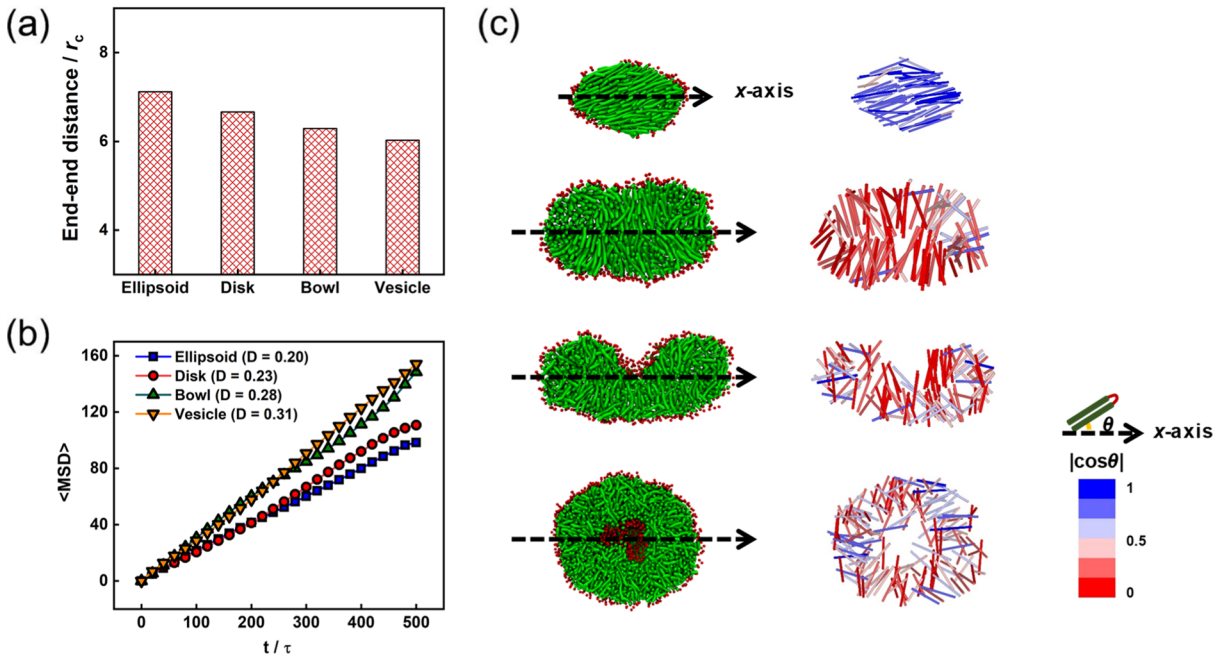

Figure 4. Rigidity of rod blocks and mobility of copolymers. (a) Change of end−end distance during the morphology transitions. (b) MSD of the copolymer under various simulation conditions. The diffusion coefficient, D, is provided for various morphologies from ellipsoids to vesicles. (c) Arrangement of rod blocks in the morphologies. Left: the representative cross-sectional slices of the ellipsoid, disk, bowl, and vesicle, respectively. Right: the detailed arrangement of the rod blocks. The direction of rod blocks is measured by the angle θ between the x-axis and the normalized vectors of rod blocks. The colors range from blue (rod block arranges along the x-axis) to red (rod block arranges perpendicular to the x-axis).

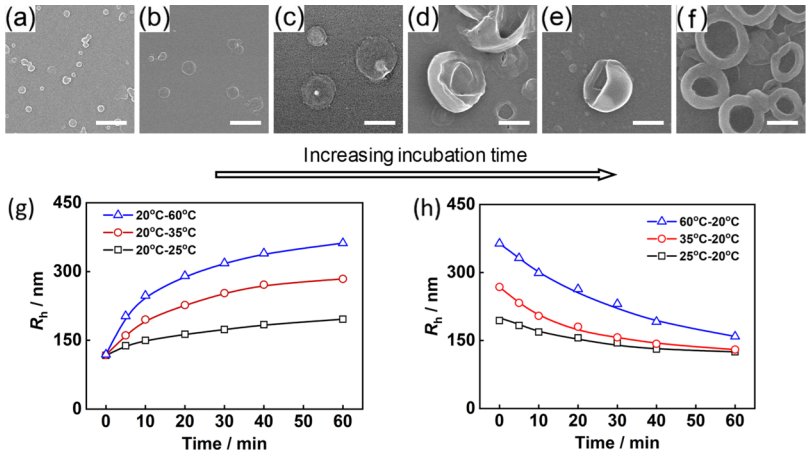

Figure 5. Morphology transition kinetics from ellipses to vesicles with different temperature programs. (a) Ellipsoids self-assembled from BEB copolymers at 20 °C. (b−f) SEM images obtained by changing the solution temperature to 60 °C directly and then incubating for various times: (b) 5, (c) 10, (d) 20, (e) 30, and (f) 60 min. (g,h) Temporal variation of R_h with different temperature programs: (g) ellipsoids are formed at 20 °C, and the solutions are subjected to 25, 35, and 60 °C, respectively, (h) solutions are quenched back to 20 °C from 25, 35, and 60 °C. Scales bars = 500 nm.

energy (E_{tol}) is the pairwise interaction energy between the solvent beads and the beads of copolymers in the aggregates. E_{tol} can be divided into two parts, that is, the interaction between coil blocks and solvent (E_{CS}) and the interaction between rod blocks and solvent (E_{RS}). As shown in Figure 3d, E_{tol} decreases during the process of morphology transitions which indicates that the copolymers undergo an energy-favorable pathway. The decrease of E_{tol} is contributed by the decrease of both E_{CS} and E_{RS}, which is because both coil blocks and rod blocks tend to stay in a stable state. The above results reveal that the behavior of aggregation, fusion, and closure is energy-favorable.

Knowing the detailed changes of mobility and rigidity is important to understand the temperature-induced morphology transitions. The end-to-end distance of rod blocks and the mean-square displacement (MSD) of rod-coil-rod triblock copolymers were evaluated to examine the variation of rigidity and mobility of copolymers, respectively. Because the end-to-end distance of rod blocks is related to the chain stiffness, and larger D means that polymer chains have a greater ability to move (*i.e.*, MSD ∼ Dt, where D is the diffusion coefficient). As shown in Figure 4a, the end-to-end distance of rod blocks decreases gradually during the ellipsoid-disk-bowl-vesicle morphology transition. This means the rigidity of rod blocks decreases. Figure 4b shows that the D values of rod-coil-rod

https://dx.doi.org/10.1021/acs.langmuir.0c03644
Langmuir 2021, 37, 3148−3157

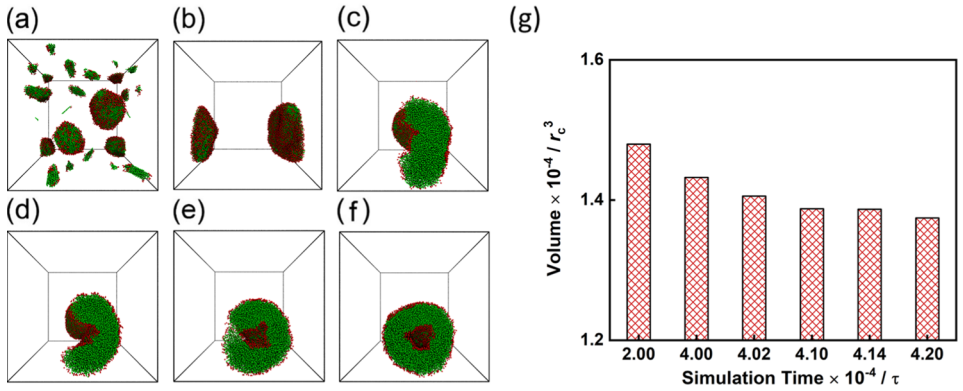

Figure 6. Kinetics of morphology transition in the simulation. (a–f) Typical snapshots during the morphology transitions: (a) 2.00×10^4 τ, (b) 4.00×10^4 τ, (c) 4.02×10^4 τ, (d) 4.10×10^4 τ, (e) 4.14×10^4 τ, and (f) 4.20×10^4 τ, where $k_BT = 0.99$, $k_c = 50$ at the beginning and then changes to $k_BT = 1.11$, $k_c = 40$ after 2.0×10^4 τ. (g) Volume changes during the transition process.

triblock copolymers in the ellipsoid, disk, bowl, and vesicle aggregates have obvious sequential increases. The copolymers at higher temperatures have greater mobility which can influence the arrangement of rod-coil-rod copolymers in assemblies.

The arrangement manner of copolymer chains is accordingly investigated. Four representative cross-sectional slices of these assemblies are shown in Figure 4c. The arrangement of the rod blocks in these cross-sectional slices is exhibited. We also measure the direction of rod blocks which is manifested by the absolute value of cosine of the orientation angle ($|\cos \theta|$) between the x-axis and the normalized vectors of rod blocks. The rod blocks in ellipsoid arrange basically along the x-axis and then turn to arrange mainly perpendicular to the x-axis in the disk, forming an oblate structure. Due to invagination, the arrangement of rod blocks starts to become less organized and the oblate bilayer structure curves. When the bowl closes, the rod blocks in vesicles are not evenly arranged around the circle, indicating that the rod blocks are relatively disordered. Typical density profiles of the rod blocks, as well as coil blocks along the long axis of the bowls and vesicles, are shown in Figure S6.

The above theoretical results confirm that due to the increase of temperature, the thermal energy leads to an increase in the mobility of copolymer chains and a decrease in the rigidity of rod blocks simultaneously. Both the increase of mobility and the decrease of the rigidity of copolymers change the arrangements of rod-coil-rod triblock copolymers, inducing transitions from ellipsoids to vesicles.

Kinetics of Morphology Transition. To study the temporal evolution of assembly morphologies, we prepared assemblies by adding 3 mL of water to 10 mL of PBLG-*b*-PEG-*b*-PBLG solution in THF (0.1 g/L) at 20 °C. Then, the solution was directly subjected to 60 °C (no dialysis was conducted). At set intervals within the annealing process, the sample solution (0.5 mL) was pipetted into 10 mL of deionized water to freeze the aggregate morphology. The morphology transition process is captured by SEM. As shown in Figure 5a, ellipsoids are formed at 20 °C. When incubating at 60 °C, aggregate morphology transitions against time are observed. After incubating for 5 min, the ellipsoids fuse into small disk-like structures (Figure 5b). With increasing the incubating time, the disk-like micelles fuse to form larger disk-like micelles (10 min, Figure 5c). The disk-like micelles bend (20 min, Figure 5d) into bowl-like structures (30 min, Figure 5e). Finally, vesicles are formed (60 min, Figure 5f). Further increasing the incubating time exerts no apparent influence on the aggregate morphology; the whole transition process is finished within 1 h. A reverse morphology transition process, that is, from the vesicle to disk then to ellipsoids can be observed by cooling the solution from 60 to 20 °C. Additionally, the solution prepared at 20 °C was also subjected to 25 and 35 °C, respectively. The temporal evolution of aggregate morphologies shows that disks or bowls can be found instead of vesicles in the same incubation period. Detailed SEM images are shown in Figure S5.

We also measured the R_h of BEB copolymer assemblies *in situ* to monitor the kinetic morphology transition in solution. Figure 5g shows the temporal variation of R_h at different incubation temperatures. BEB assemblies are first prepared at 20 °C and then subjected to 25, 35, and 60 °C respectively. During the incubation, R_h of BEB assemblies increases. At the same incubation time, R_h is larger at higher incubation temperatures. When the morphology transition is completed, the R_h of BEB assemblies is different, which also indicates that various intermediate morphologies are stable at the corresponding temperature. Additionally, Figure 5h presents the corresponding cooling process. By quenching the temperature from 60, 35, and 25 °C back to 20 °C, respectively, the R_h of BEB assemblies decreases. However, the R_h of all the BEB assemblies cannot completely turn back to its original value. Combining with SEM results, this phenomenon is ascribed to the fact that the disk-like structures are difficult to fully disassemble into ellipsoids once they form.

To mimic this kinetic process in DPD simulations, we set the simulation settings from $k_BT = 0.99$, $k_c = 50$ to $k_BT = 1.11$, $k_c = 40$ directly corresponding to the experimental settings in the experiments (*i.e.*, 20–60 °C). The morphology transitions can be observed over time. Figure 6a–f show the detailed transition processes. Ellipsoids are first observed at low temperature. After the changes in simulation conditions, the formed primary micelles get close and fuse into disks. Then, bowls emerge and vesicles form as the simulation continues. To monitor the morphology transition process, the volume variation of these aggregates during morphology transitions is calculated. The volume is the quantity of the three-dimensional space enclosed by a closed surface. In the simulations, the volume of aggregates was obtained by calculating the number of simulation box lattices occupied by the aggregates. As shown in Figure 6g, the volume of six typical assemblies decreases gradually. It is attributed to the aggregation, fusion, and closure

https://dx.doi.org/10.1021/acs.langmuir.0c03644
Langmuir 2021, 37, 3148–3157

behaviors. Due to the aggregation of polymer chains, the self-assembly of copolymers and the fusion of assembles decrease the occupied volume. The closure of disks causes a slight change in the volume because no obvious stretching or compression occurs.[57]

Distinct Transition Pathway of Rod-Coil Block Copolymer Assemblies. For the formation of vesicles from the coil−coil system, the dynamic morphology transition process usually undergoes a sphere−cylinder−lamellae−vesicle transition, which is well-known as the cone−column mechanism.[52−54] For example, poly(styrene-*b*-isoprene) (PS-*b*-PI) copolymers can self-assemble into spheres in solution, and the micellar morphology changes from spheres to cylinders to vesicles in response to the change of environmental conditions.[52] However, through the present experiments and simulations, we found that the disks appear instead of cylinder structures during the morphology transition process of the rod-coil system. That is, the rod-coil system has a different morphology transition pathway from the coil−coil system. In the case of the coil−coil block copolymer assemblies, the morphology transition is governed by three dominant contributions including the interactions of solvated corona blocks, the interfacial tension between the micelle core and surrounding solvent, and the stretching of the core blocks.[53,54] Due to the repulsive interaction between the hydrophobic block and the solvent, the flexible copolymer chains tend to form small spheres. To reduce the interfacial tension, spheres favor to form short rods, and the high end-cap energies drive the short rods to form long rods (cylinders).[55,56] Then, the cylinders fuse into lamellae to reduce the interface tension. After the formation of this structure, the lamellae curves and vesicles form easily because the bending energy is weak.

In contrast, the core blocks in the rod-coil system are rigid, which means that the copolymer chains are relatively extended. Compared to the coil−coil system, the rod-coil system is more difficult to form spheres or short rod morphologies because the alignment of hydrophobic rod blocks has a significant impact on the morphologies. In the present work, the rod-coil-rod copolymers first self-assemble into ellipsoids to minimize the defects in the arrangement of hydrophobic rod blocks.[57] The formed ellipsoids fuse into disks which can minimize the interfacial contact between the solvent and the hydrophobic rod blocks in an energy favorable way. To reduce the edge energy, the disks close and vesicles form once the bending energy decreases.

To deepen the understanding of the mechanism, the morphology transitions of triblock copolymers with coil hydrophobic blocks ($\mathbf{A}_{12}\mathbf{C}_4\mathbf{A}_{12}$, **A** denotes the coil hydrophobic block) are also examined by simulations. The results are presented in Figure S7. The simulation parameter settings are the same as the $\mathbf{R}_{12}\mathbf{C}_4\mathbf{R}_{12}$ system. The copolymers with hydrophobic coil blocks form small vesicles at 20 °C (Figure S7). By careful examination, we find that the formation of vesicles follows a sphere-cylinder-lamellae-vesicle morphology transition, which is consistent with the results reported in the literature.[52] Such a pathway is significantly different from the ellipsoid-disk-bowl-vesicle transition process of the rod-coil systems.

We also investigate the effect of rod block length on the morphology transition process for the rod-coil systems. Rod-coil-rod copolymers with various lengths of rod hydrophobic blocks ($\mathbf{R}_8\mathbf{C}_4\mathbf{R}_8$ and $\mathbf{R}_{16}\mathbf{C}_4\mathbf{R}_{16}$) are examined, and the results are presented in Figure S8. For the rod-coil system, the longer hydrophobic rod blocks have a high degree of chain ordering, which greatly influences the arrangement of copolymers and enhances the stability of self-assembled oblate bilayers (Figure S8). Thus, $\mathbf{R}_{16}\mathbf{C}_4\mathbf{R}_{16}$ only forms large disks instead of vesicles with temperature increases. While the copolymers with shorter hydrophobic rod blocks ($\mathbf{R}_8\mathbf{C}_4\mathbf{R}_8$) form vesicles easily than $\mathbf{R}_{12}\mathbf{C}_4\mathbf{R}_{12}$, the reason is that shorter hydrophobic rod blocks have greater mobility and less chain rigidity, which decreases the chain ordering of rod blocks. These results further verify that the chain ordering of rod blocks in the rod-coil assemblies plays an important role in the assembly morphologies, which well supports the proposed mechanism.

CONCLUSIONS

In summary, an ellipsoid−disk−bowl−vesicle morphology transition of PBLG-*b*-PEG-*b*-PBLG polypeptide-based triblock copolymers in response to temperature was found from experiments and DPD simulations. At room temperature, the polypeptide copolymers self-assemble into ellipsoids. By increasing the temperature, the ellipsoids first fuse into disk-like structures and then wrap up into vesicles. During the morphology transition process, the chain mobility increases and the chain rigidity decreases by increasing the temperature, which results in the change of PBLG block ordering. The variation of chain ordering induces an ellipsoid-to-vesicle morphology transition, which exhibits a difference in contrast to the coil−coil block copolymer system. This programmable morphology transition shows a distinct transition pathway of rod-coil copolymer assemblies, and the obtained results can guide the precise control of the nanoassembly morphologies.

ASSOCIATED CONTENT

Supporting Information

The Supporting Information is available free of charge at https://pubs.acs.org/doi/10.1021/acs.langmuir.0c03644.

Full experimental details including synthesis and characterization of triblock copolymers; SEM, TEM, and AFM images; DLS and CD results; and DPD simulation details (PDF).

AUTHOR INFORMATION

Corresponding Authors

Jiaping Lin − *Shanghai Key Laboratory of Advanced Polymeric Materials, Key Laboratory for Ultrafine Materials of Ministry of Education, Frontiers Science Center for Materiobiology and Dynamic Chemistry, School of Materials Science and Engineering, East China University of Science and Technology, Shanghai 200237, China;* orcid.org/0000-0001-9633-4483; Email: jlin@ecust.edu.cn

Chunhua Cai − *Shanghai Key Laboratory of Advanced Polymeric Materials, Key Laboratory for Ultrafine Materials of Ministry of Education, Frontiers Science Center for Materiobiology and Dynamic Chemistry, School of Materials Science and Engineering, East China University of Science and Technology, Shanghai 200237, China;* orcid.org/0000-0001-9008-6327; Email: caichunhua@ecust.edu.cn

Authors

Xiao Jin − *Shanghai Key Laboratory of Advanced Polymeric Materials, Key Laboratory for Ultrafine Materials of Ministry of Education, Frontiers Science Center for Materiobiology and Dynamic Chemistry, School of Materials Science and*

https://dx.doi.org/10.1021/acs.langmuir.0c03644
Langmuir 2021, 37, 3148−3157

Engineering, East China University of Science and Technology, Shanghai 200237, China

Fangsheng Wu − *Shanghai Key Laboratory of Advanced Polymeric Materials, Key Laboratory for Ultrafine Materials of Ministry of Education, Frontiers Science Center for Materiobiology and Dynamic Chemistry, School of Materials Science and Engineering, East China University of Science and Technology, Shanghai 200237, China*

Liquan Wang − *Shanghai Key Laboratory of Advanced Polymeric Materials, Key Laboratory for Ultrafine Materials of Ministry of Education, Frontiers Science Center for Materiobiology and Dynamic Chemistry, School of Materials Science and Engineering, East China University of Science and Technology, Shanghai 200237, China;* orcid.org/0000-0002-5141-8584

Jianding Chen − *Shanghai Key Laboratory of Advanced Polymeric Materials, Key Laboratory for Ultrafine Materials of Ministry of Education, Frontiers Science Center for Materiobiology and Dynamic Chemistry, School of Materials Science and Engineering, East China University of Science and Technology, Shanghai 200237, China*

Liang Gao − *Shanghai Key Laboratory of Advanced Polymeric Materials, Key Laboratory for Ultrafine Materials of Ministry of Education, Frontiers Science Center for Materiobiology and Dynamic Chemistry, School of Materials Science and Engineering, East China University of Science and Technology, Shanghai 200237, China*

Complete contact information is available at: https://pubs.acs.org/10.1021/acs.langmuir.0c03644

Author Contributions

†X.J. and F.W. contributed equally to this work.

Notes

The authors declare no competing financial interest.

■ ACKNOWLEDGMENTS

This work was supported by the National Natural Science Foundation of China (51833003, 51621002, and 21975073). Support from project of Shanghai municipality (20ZR1471300) is also appreciated.

■ REFERENCES

(1) Shi, K.; Cui, F.; Bi, H.; Jiang, Y.; Song, T. Polycationic Peptide Guided Spherical Ordered Self-Assembly of Biomacromolecules. *Biomaterials* **2012**, *33*, 8723−8732.

(2) Xu, B.; Feng, C.; Huang, X. A Versatile Platform for Precise Synthesis of Asymmetric Molecular Brush in One Shot. *Nat. Commun.* **2017**, *8*, 333−340.

(3) Machado, C. A.; Smith, I. R.; Savin, D. A. Self-Assembly of Oligo- and Polypeptide-Based Amphiphiles: Recent Advances and Future Possibilities. *Macromolecules* **2019**, *52*, 1899−1911.

(4) Feng, C.; Huang, X. Polymer Brushes: Efficient Synthesis and Applications. *Acc. Chem. Res.* **2018**, *51*, 2314−2323.

(5) Xu, B.; Feng, C.; Hu, J.; Shi, P.; Gu, G.; Wang, L.; Huang, X. Spin-Casting Polymer Brush Films for Stimuli-Responsive and Anti-Fouling Surfaces. *ACS Appl. Mater. Interfaces* **2016**, *8*, 6685−6692.

(6) Zhang, X.; Wang, L.; Xu, J.; Chen, D.; Shi, L.; Zhou, Y.; Shen, Z. Polymeric Supramolecular Systems: Design, Assembly and Functions. *Acta Polym. Sin.* **2019**, *50*, 973−987.

(7) Ye, Q.; Huo, M.; Zeng, M.; Liu, L.; Peng, L.; Wang, X.; Yuan, J. Photoinduced Reversible Worm-to-Vesicle Transformation of Azo-Containing Block Copolymer Assemblies Prepared by Polymerization-Induced Self-Assembly. *Macromolecules* **2018**, *51*, 3308−3314.

(8) Zheng, Y.; Weng, C.; Cheng, C.; Zhao, J.; Yang, R.; Zhang, Q.; Ding, M.; Tan, H.; Fu, Q. Multiblock Copolymers toward Segmentation-Driven Morphological Transition. *Macromolecules* **2020**, *53*, 5992−6001.

(9) Molla, M. R.; Rangadurai, P.; Antony, L.; Swaminathan, S.; de Pablo, J. J.; Thayumanavan, S. Dynamic Actuation of Glassy Polymersomes through Isomerization of a Single Azobenzene Unit at the Block Copolymer Interface. *Nat. Chem.* **2018**, *10*, 659−666.

(10) Que, Y.; Liu, Y.; Tan, W.; Feng, C.; Shi, P.; Li, Y.; Xiaoyu, H. Enhancing Photodynamic Therapy Efficacy by Using Fluorinated Nanoplatform. *ACS Macro Lett.* **2016**, *5*, 168−173.

(11) Tao, D.; Feng, C.; Cui, Y.; Yang, X.; Manners, I.; Winnik, M. A.; Huang, X. Monodisperse Fiber-like Micelles of Controlled Length and Composition with an Oligo(*p*-phenylenevinylene) Core via "Living" Crystallization-Driven Self-Assembly. *J. Am. Chem. Soc.* **2017**, *139*, 7136−7139.

(12) Shen, L.; Du, J.; Armes, S. P.; Liu, S. Kinetics of pH-Induced Formation and Dissociation of Polymeric Vesicles Assembled from a Water-Soluble Zwitterionic Diblock Copolymer. *Langmuir* **2008**, *24*, 10019−10025.

(13) Meeuwissen, S. A.; Kim, K. T.; Chen, Y.; Pochan, D. J.; van Hest, J. C. M. Controlled Shape Transformation of Polymersome Stomatocytes. *Angew. Chem., Int. Ed.* **2011**, *50*, 7070−7073.

(14) Kim, K. T.; Zhu, J.; Meeuwissen, S. A.; Cornelissen, J. J. L. M.; Pochan, D. J.; Nolte, R. J. M.; van Hest, J. C. M. Polymersome Stomatocytes: Controlled Shape Transformation in Polymer Vesicles. *J. Am. Chem. Soc.* **2010**, *132*, 12522−12524.

(15) Nishimura, T.; Shishi, S.; Sasaki, Y.; Akiyoshi, K. Thermoresponsive Polysaccharide Graft Polymer Vesicles with Tunable Size and Structural Memory. *J. Am. Chem. Soc.* **2020**, *142*, 11784−11790.

(16) Antonietti, M.; Förster, S. Vesicles and Liposomes: A Self-Assembly Principle Beyond Lipids. *Adv. Mater.* **2003**, *15*, 1323−1333.

(17) Derry, M. J.; Mykhaylyk, O. O.; Armes, S. P. A Vesicle-to-Worm Transition Provides a New High-Temperature Oil Thickening Mechanism. *Angew. Chem., Int. Ed.* **2017**, *56*, 1746−1750.

(18) Wang, S.; Shen, Y.; Zhang, J.; Xu, S.; Liu, H. A Designed Lipopeptide with a Leucine Zipper as an Imbedded on/off Switch for Lipid Bilayers. *Phys. Chem. Chem. Phys.* **2016**, *18*, 10129−10137.

(19) Moughton, A. O.; Patterson, J. P.; O'Reilly, R. K. Reversible Morphological Switching of Nanostructures in Solution. *Chem. Commun.* **2011**, *47*, 355−357.

(20) Cai, Y.; Aubrecht, K. B.; Grubbs, R. B. Thermally Induced Changes in Amphiphilicity Drive Reversible Restructuring of Assemblies of ABC Triblock Copolymers with Statistical Polyether Blocks. *J. Am. Chem. Soc.* **2011**, *133*, 1058−1065.

(21) Dai, W.; Zhu, X.; Zhang, J.; Zhao, Y. Temperature and Solvent Isotope Dependent Hierarchical Self-Assembly of a Heterografted Block Copolymer. *Chem. Commun.* **2019**, *55*, 5709−5712.

(22) Sundararaman, A.; Stephan, T.; Grubbs, R. B. Reversible Restructuring of Aqueous Block Copolymer Assemblies through Stimulus-Induced Changes in Amphiphilicity. *J. Am. Chem. Soc.* **2008**, *130*, 12264−12265.

(23) Bhargava, P.; Tu, Y.; Zheng, J. X.; Xiong, H.; Quirk, R. P.; Cheng, S. Z. D. Temperature-Induced Reversible Morphological Changes of Polystyrene-*block*-Poly(Ethylene Oxide) Micelles in Solution. *J. Am. Chem. Soc.* **2007**, *129*, 1113−1121.

(24) Zhang, J.; Lin, W.; Liu, A.; Yu, Z.; Wan, X.; Liang, D.; Zhou, Q. Solvent Effect on the Aggregation Behavior of Rod−Coil Diblock Copolymers. *Langmuir* **2008**, *24*, 3780−3786.

(25) Yang, C.; Gao, L.; Lin, J.; Wang, L.; Cai, C.; Wei, Y.; Li, Z. Toroid Formation through a Supramolecular "Cyclization Reaction" of Rodlike Micelles. *Angew. Chem., Int. Ed.* **2017**, *56*, 5546−5550.

(26) Yang, C.; Li, Q.; Cai, C.; Lin, J. Nanoparticle-Induced Ellipse-to-Vesicle Morphology Transition of Rod−Coil−Rod Triblock Copolymer Aggregates. *Langmuir* **2016**, *32*, 6917−6927.

(27) Ding, W.; Lin, S.; Lin, J.; Zhang, L. Effect of Chain Conformation Change on Micelle Structures: Experimental Studies and Molecular Dynamics Simulations. *J. Phys. Chem. B* **2008**, *112*, 776−783.

(28) Cai, C.; Lin, J.; Lu, Y.; Zhang, Q.; Wang, L. Polypeptide Self-Assemblies: Nanostructures and Bioapplications. *Chem. Soc. Rev.* **2016**, *45*, 5985−6012.
(29) Zhuang, Z.; Cai, C.; Jiang, T.; Lin, J.; Yang, C. Self-Assembly Behavior of Rod−Coil−Rod Polypeptide Block Copolymers. *Polymer* **2014**, *55*, 602−610.
(30) Guan, Z.; Liu, D.; Lin, J.; Wang, X. Aqueous Self-Assembly of Hydrophobic Macromolecules with Adjustable Rigidity of the Backbone. *Soft Matter* **2017**, *13*, 5130−5136.
(31) Liu, H.; Wang, R.; Wei, J.; Cheng, C.; Zheng, Y.; Pan, Y.; He, X.; Ding, M.; Tan, H.; Fu, Q. Conformation-Directed Micelle-to-Vesicle Transition of Cholesterol-Decorated Polypeptide Triggered by Oxidation. *J. Am. Chem. Soc.* **2018**, *140*, 6604−6610.
(32) Huo, M.; Song, G.; Zhang, J.; Wei, Y.; Yuan, J. Nonspherical Liquid Crystalline Assemblies with Programmable Shape Transformation. *ACS Macro Lett.* **2018**, *7*, 956−961.
(33) Han, L.; Wang, M.; Jia, X.; Chen, W.; Qian, H.; He, F. Uniform two-dimensional square assemblies from conjugated block copolymers driven by $\pi-\pi$ interactions with controllable sizes. *Nat. Commun.* **2018**, *9*, 865−876.
(34) Uematsu, I.; Uematsu, Y. Polypeptide liquid crystals. *Adv. Polym. Sci.* **1984**, *59*, 37−73.
(35) Cai, C.; Lin, J.; Zhuang, Z.; Zhu, W. Ordering of Polypeptides in Liquid Crystals, Gels and Micelles. *Adv. Polym. Sci.* **2013**, *259*, 159−199.
(36) Yakubovich, A. V.; Solov'yov, I. A.; Solov'yov, A. V.; Greiner, W. Phase Transition in Polypeptides: a Step Towards the Understanding of Protein Folding. *Eur. Phys. J. D* **2006**, *40*, 363−367.
(37) Han, Y.; Yu, H.; Du, H.; Jiang, W. Effect of Selective Solvent Addition Rate on the Pathways for Spontaneous Vesicle Formation of ABA Amphiphilic Triblock Copolymers. *J. Am. Chem. Soc.* **2010**, *132*, 1144−1150.
(38) Solov'yov, I. A.; Yakubovich, A. V.; Solov'yov, A. V.; Greiner, W. α-Helix↔Random Coil Phase Transition: Analysis of ab Initio Theorypredictions. *Eur. Phys. J. D* **2008**, *46*, 227−240.
(39) Su, Y.-j.; Huang, J.-h. Self-Assembly Behavior of Rod-Coil-Rod Triblock Copolymers Within a Planar Slit. *Chin. J. Polym. Sci.* **2016**, *34*, 838−849.
(40) Groot, R. D.; Warren, P. B. Dissipative Particle Dynamics: Bridging the Gap between Atomistic and Mesoscopic Simulation. *J. Chem. Phys.* **1997**, *107*, 4423−4435.
(41) Hoogerbrugge, P. J.; Koelman, J. M. V. A. Simulating Microscopic Hydrodynamic Phenomena with Dissipative Particle Dynamics. *Europhys. Lett.* **1992**, *19*, 155−160.
(42) Xu, Z.; Lin, J.; Zhang, Q.; Wang, L.; Tian, X. Theoretical Simulations of Nanostructures Self-Assembled from Copolymer Systems. *Polym. Chem.* **2016**, *7*, 3783−3811.
(43) Zhang, Q.; Lin, J.; Wang, L.; Xu, Z. Theoretical Modeling and Simulations of Self-Assembly of Copolymers in Solution. *Prog. Polym. Sci.* **2017**, *75*, 1−30.
(44) Sepehr, F.; Paddison, S. J. Dissipative Particle Dynamics Interaction Parameters from ab Initio Calculations. *Chem. Phys. Lett.* **2016**, *645*, 20−26.
(45) Li, X.-x.; Gu, M.; Zhang, L.; Lin, J. Computational Investigation on the Superstructures of Micelles from Amphiphilic DNA Block Copolymers. *Acta Polym. Sin.* **2020**, *51*, 1257−1266.
(46) Yu, C.-y.; Li, S.-l.; Li, K.; Zhou, Y. Investigation of the Transformation Dynamics of Diblock Copolymers Assemblies in Reverse Solvent via Computer Simulation. *Acta Polym. Sin.* **2020**, *51*, 311−318.
(47) de Meyer, F. J.-M.; Rodgers, J. M.; Willems, T. F.; Smit, B. Molecular Simulation of the Effect of Cholesterol on Lipid-Mediated Protein-Protein Interactions. *Biophys. J.* **2010**, *99*, 3629−3638.
(48) Venturoli, M.; Smit, B.; Sperotto, M. M. Simulation Studies of Protein-Induced Bilayer Deformations, and Lipid-Induced Protein Tilting, on a Mesoscopic Model for Lipid Bilayers with Embedded Proteins. *Biophys. J.* **2005**, *88*, 1778−1798.
(49) Li, Z.; Tang, Y.-H.; Lei, H.; Caswell, B.; Karniadakis, G. E. Energy-Conserving Dissipative Particle Dynamics with Temperature-Dependent Properties. *J. Comput. Phys.* **2014**, *265*, 113−127.
(50) Xiao, M.; Xia, G.; Wang, R.; Xie, D. Controlling the Self-Assembly Pathways of Amphiphilic Block Copolymers into Vesicles. *Soft Matter* **2012**, *8*, 7865−7874.
(51) Kuo, S.-W.; Lee, H.-F.; Huang, C.-F.; Huang, C.-J.; Chang, F.-C. Synthesis and Self-Assembly of Helical Polypeptide-Random Coil Amphiphilic Diblock Copolymer. *J. Polym. Sci., Part A: Polym. Chem.* **2008**, *46*, 3108−3119.
(52) Bang, J.; Jain, S.; Li, Z.; Lodge, T. P.; Pedersen, J. S.; Kesselman, E.; Talmon, Y. Sphere, Cylinder, and Vesicle Nanoaggregates in Poly(styrene-*b*-isoprene) Diblock Copolymer Solutions. *Macromolecules* **2006**, *39*, 1199−1208.
(53) Mai, Y.; Eisenberg, A. Self-Assembly of Block Copolymers. *Chem. Soc. Rev.* **2012**, *41*, 5969−5985.
(54) Chen, C.; Wylie, R. A. L.; Klinger, D.; Connal, L. A. Shape Control of Soft Nanoparticles and Their Assemblies. *Chem. Mater.* **2017**, *29*, 1918−1945.
(55) Shen, H.; Eisenberg, A. Morphological Phase Diagram for a Ternary System of Block Copolymer PS_{310}-b-PAA_{52}/Dioxane/H_2O. *J. Phys. Chem. B* **1999**, *103*, 9473−9487.
(56) Rumyantsev, A. M.; Leermakers, F. A. M.; Zhulina, E. B.; Potemkin, I. I.; Borisov, O. V. Temperature-Induced Re-Entrant Morphological Transitions in Block-Copolymer Micelles. *Langmuir* **2019**, *35*, 2680−2691.
(57) Olsen, B.; Segalman, R. Self-Assembly of Rod−Coil Block Copolymers. *Mater. Sci. Eng., R* **2008**, *62*, 37−66.

https://dx.doi.org/10.1021/acs.langmuir.0c03644
Langmuir 2021, 37, 3148−3157